Crack growth rates of Inconel 600 in aqueous solutions at elevated temperature

E. A. ASHOUR
National Research Centre, Physical Chemistry Department, Dokki, Cairo, Egypt
E-mail: eaashour@mailcity.com

The effect of sulfate ions on the crack growth rates (CGRs) of notched specimens (CT) of Inconel 600 under constant load has been investigated in chloride containing aqueous solutions at 250 °C. The intergranular stress corrosion crack growth rates increased in chloride solutions while its hinder with increasing sulfate concentrations. Stress intensity factor (k) for stress corrosion cracking decreased with increasing of aggressivity of chloride ions while increased in the presence of sulfate solutions. At very low concentration of chloride (0.001 m), k-value retardation was observed. It is clear from the results that hydrogen in the aqueous solutions has a deleterious effect on crack propagation. The difference in crack growth rates in chloride ions and in chloride containing sulfate solution at high temperature can be recognized as caused by the difference in local environment conditions at a crack tip. The results indicate that the crack don't propagate under this conditions in the presence of sulfate ions. It is mainly due to a hinderance of chloride ions adsorption on active sites of the fracture surfaces and the formation of chromium oxide layer which is stable at higher temperature. © *2001 Kluwer Academic Publishers*

1. Introduction

It is well known that Inconel 600 is susceptible to intergranular stress corrosion cracking (IGSCC) in chloride solution and in chloride with relatively low concentration of sulfate ions containing aqueous solution at elevated temperature with different constant extension rates [1]. Although the most important investigation in the previous part I to prevent the occurrence of crack initiation, it is also necessary to investigate the crack propagation rate of IGSCC in this relevant media. On the other hand, scc of stainless steel 304- CT samples in simulated light water reactor (LWR) conditions containing impurities at different test temperatures has been observed when different chemical and electrochemical conditions existing at the crack tip and in the bulk solution are favourable to enhance the crack growth [2]. Additionally, it has been reported [3, 4] that a sulfur content in hot water is able to simulate the growth of chloride induced pits and cracks on stainless steel Type AISI 321. That means, in hot water of 250 °C sulfate could be able to act as an oxidant and therefore to promote the metal dissolution in pits and crevices [3, 4]. That also the onset of scc of stainless steel Type AISI 321 is due to the hydrogen content of the cathodic corrosion reactions inside the crack which affected crack propagation process on the base of local hydrogen embrittlement [5–7]. It is not possible to isolate an anodic dissolution type of mechanism from a hydrogen related mechanism of cracking and it is also known that Alloy 600 is susceptible to cracking when it is polarized cathodically [8]. Crack growth rate (CGR) is strongly influenced by the temperature.

There is evidence that IGSCC cannot be nucleated or propagated in Alloy 600 below a critical temperature (Tcrit $\cong$ 250°C) [9, 10]. Above Tcrit, CGR increases as the temperature increases. The influencing of loading and in particular of the stress intensity factor K_I on Alloy 600 are limited data [11–14]. This aspect needs further investigation.

The plan for the present work on crack growth rates (CGRs) for Alloy 600 tested under constant load conditions in aqueous solutions at 250°C was based on an earlier investigations of initiation and inhibition of corrosion cracking process [1]. This paper follows the two previous parts of this program in this series on Inconel 600 [1,15]. Crack growth rate is very important for life prediction of high alloyed materials used in power and chemical industries.

2. Experimental procedure
2.1. Materials
Side- grooved compact type specimens (CT) were machined from Inconel 600 whose chemical composition and mechanical properties are listed in Tables I and II.

2.2. Specimens
Subsize side – grooved compact tension type specimens were subjected to fatigue loading to form a precrack according to the specifications given by ASTM- E 399 [16]. The dimensions of used specimen (both crack length (a) and thickness (b)) are not satisfying the relation $a, b \supseteq 2.5\,(K_{IC}/\sigma_{YS})^2$, then it is not possible to use

TABLE I Chemical composition (wt %) of the tested alloy

Alloy	Fe	Cr	Ni	Ti	Si	Mn	C	S	P	Al
Inconel 600	9.17	16.49	72.70	0.25	—	0.80	0.024	0.003	0.008	0.17

TABLE II Mechanical properties of the tested alloy

Alloy	YS[a] 0.2% at 25 °C [MPa]	YS 0.2% at 250 °C [MPa]	UTS[b] at 25 °C [MPa]	UTS at 250 °C [MPa]	Elong.% at 25 °C	Elong.% at 250 °C
Inconel 600	352	311	712	566	38.6	40.4

[a]YS = Yield strength.
[b]UTS = Ultimate tensile stress.

K_{IC} but a valid K can be used for CGR measurements instead of K_{IC} according to this method ASTM- E 399. Precracking of the specimens was carried out using a servohydraulic machine. Before testing the specimens were grinted with 280, 360, and 600 grit silicon carbide papers, degreased with ethyl alcohol and subsequently flushed with distilled water and dried.

2.3. Test solutions
The volume of solution used in autoclave was about 1500 ml. The test solutions were 0.1 m NaCl; 0.01 m NaCl; 0.001 m NaCl; 0.01 m NaCl + 0.01 m Na_2SO_4; 0.01 m NaCl + 0.1 m Na_2SO_4; 0.1 m Na_2SO_4 having an adjusted pH $\approx$ 5 at room temperature (RT). The tests have been started with air saturated solutions. The residual oxygen content depends on the testing temperature.

2.4. Temperature
250°C in an autoclave system [17]. Constant load of 7.34 and 8.39 kN (optimum condition for CGR after testing) were used in different test solutions. The investigated specimens were broken and subjected to both the measurement of crack length by optical microscope and fractographic investigations by means of scanning electron microscope (SEM).

2.5. Hydrogen determination
The hydrogen content was determined immediately at crack tip region after the mechanical tests in different test solutions by means of hot extraction equipment LECO RH 42.

3. Results and discussion
The average crack growth rates (da/dt) were determined at the open circuit potential under constant load as a function of crack length (a), the duration time of the test and stress intensity factor (k). Crack propagation is a result of the synergistic interaction of mechanical stresses and corrosion reactions. A strong dependence of crack growth on type and concentration of additive was observed. Most tests were continued to failure. Measurements of average crack growth rates were made based on ultimate crack growth and the actual test time between the onset of cracking and of failure. These data are presented in Table III. It shows calculated k-values for crack growth, average crack growth rates, aspect ratio between crack length (a) and width of tested specimen (w) i.e. a/w and the hydrogen content at the crack tip region, which was determined immediately after the mechanical tests in different test solutions under constant load (F) at 250°C. The discrepancy of the results in Table III might be due to the difference in concentrations of chloride and sulfate used. These results also suggest that crack propagation would occur once the crack was initiated. The transition from initiation to propagation was evident on the scc fracture surfaces and was marked by a change in the cracking orientation [18].

Fig. 1a–c illustrate the variation of crack length (a) with the time of tests in electrolytes with different concentrations of NaCl at 250°C under constant load at 7.34 kN. The curve pertaining to 0.001 m NaCl in Fig. 1a shows a longer crack initiation time than the curves in Fig. 1b, c pertaining to 0.01 m and 0.1 m chloride, respectively. Such a result pointed to the role that the dissolution/oxidation seems to play in crack initiation. Also it is difficult to distinguish between

TABLE III Calculated K – values and crack growth rates under constant load tests at 250°C in different test solutions

Medium	[H] (ppm)	K (MPa$\sqrt{m}$)	a/w	da/dt (mm/s)	F (kN)
0.001 m NaCl	11	326	0.85	2.31E- 05	7.34
0.01 m NaCl	10	76	0.63	6.38E- 06	7.34
0.1 m NaCl	50	88	0.67	2.00E- 05	7.34
0.001 m NaCl + 0.0001 m Na_2SO_4	—	53	0.54	2.00E- 07	8.39
0.01 m NaCl + 0.001 m Na_2SO_4	—	67	0.56	7.63E- 07	8.39
0.01 m NaCl + 0.01 m Na_2SO_4	6	59	0.54	2.00E- 07	8.39
0.01 m NaCl + 0.1 m Na_2SO_4	3	61	0.54	5.33E- 07	8.39
0.1 m Na_2SO_4	—	68	0.57	4.04E- 06	8.39
*0.1 m NaCl/0.1 m Na_2SO_4	10/3	72	0.60	2.00E- 07	8.39

*Sulfate was added by injection in the autoclave at 80°C during the growth of the crack which was started in the chloride environment at 250°C, see text.
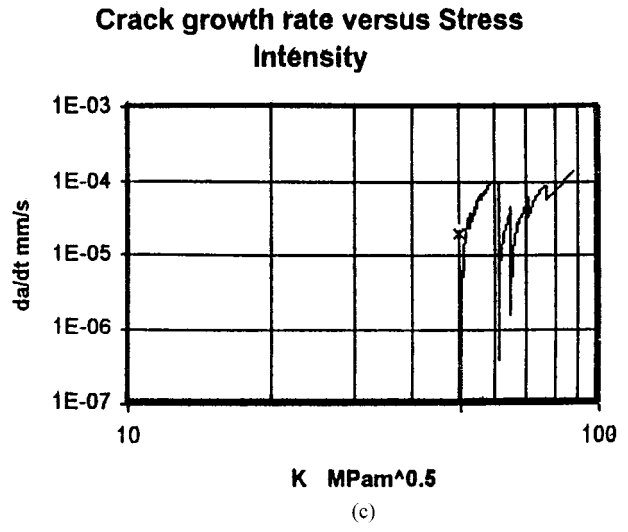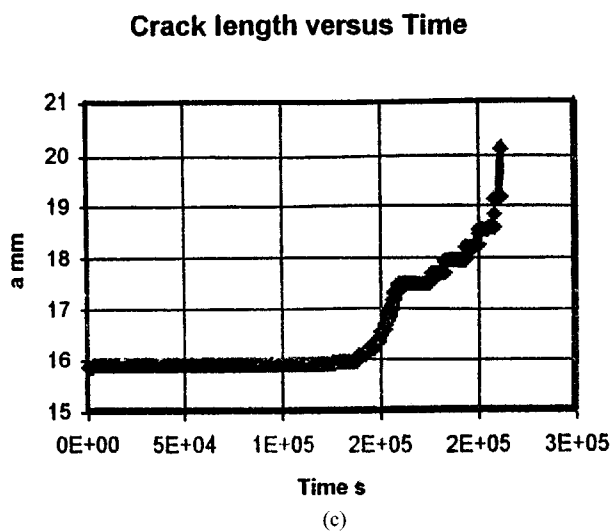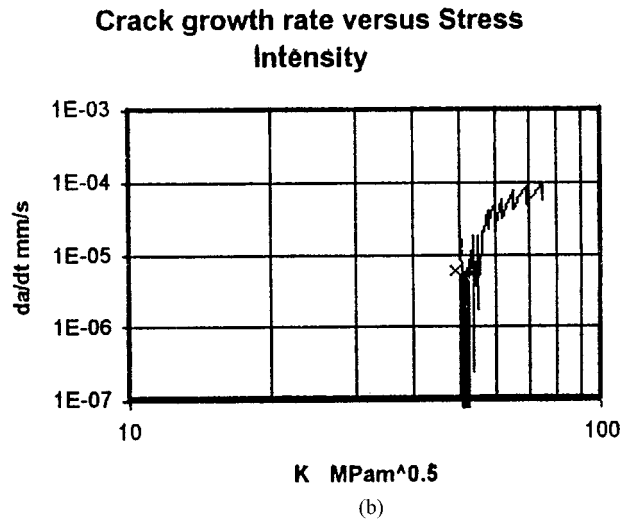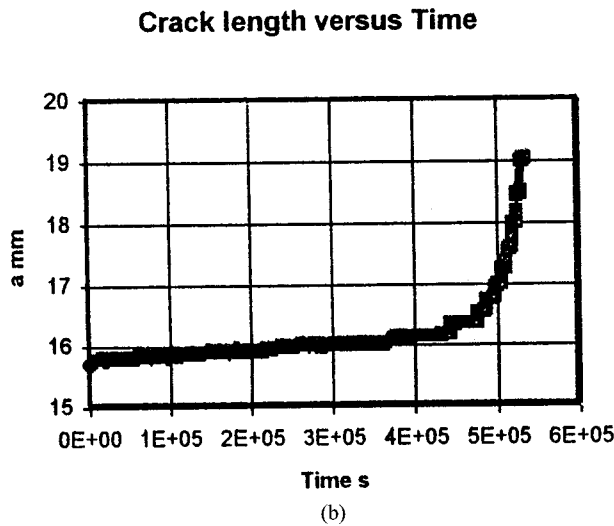
Crack length versus Time

(a)

Crack growth rate versus Stress Intensity

(a)

Crack length versus Time

(b)

Crack growth rate versus Stress Intensity

(b)

Crack length versus Time

(c)

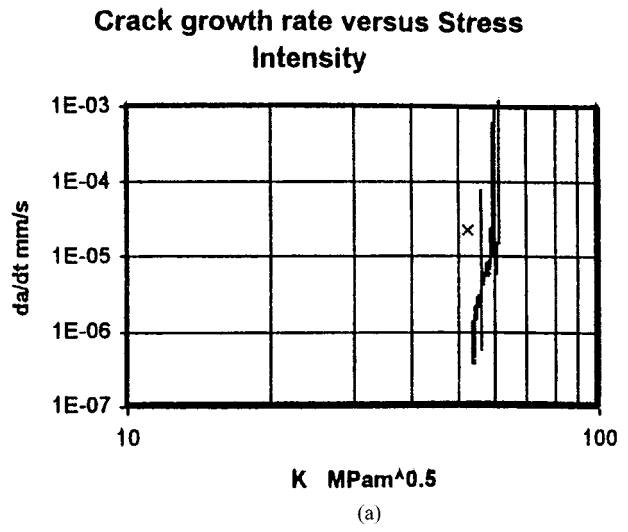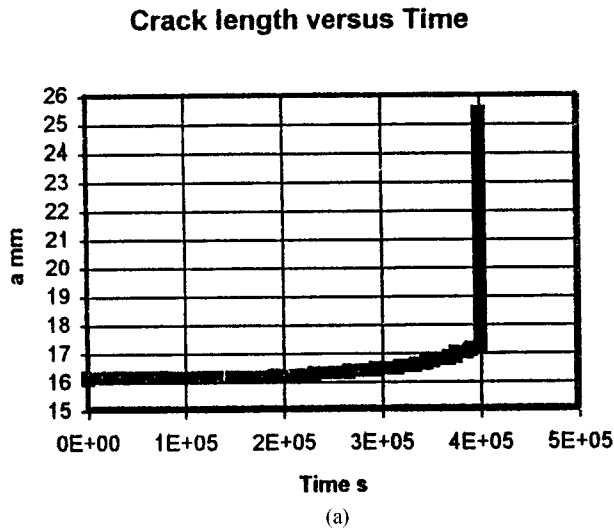**Crack growth rate versus Stress Intensity**

(c)

Figure 1 (a–c) Comparison of crack length a (mm) Vs time (s) for tests in (a) 0.001 m NaCl, (b) 0.01 m NaCl and (c) 0.1 m NaCl at 250°C under constant load at 7.34 kN.

Figure 2 (a–c) Comparison of crack growth rates Vs Kmax measured in (a) 0.001 m NaCl, (b) 0.01 m NaCl, and (c) 0.1 m NaCl at 250°C under constant load at 7.34 kN.

the crack initiation and propagation process. These two processes are dealt together in many mechanistic models of scc [8]. The crack growth rates were high once initiation occurred as shown in Fig. 2a–c. Fractographic examinations of the specimens showed that cracking mode was highly intergranular with sec-

ondary cracks and crack branching (see e.g. Figs 3–5). If stress is relatively high, cracking can continue along the grain boundaries. Increasing amounts of intergranular cracking (IG) with increasing k have been observed in many other chloride solutions [19, 20]. At very low concentrations of chloride (0.001 m), k- value
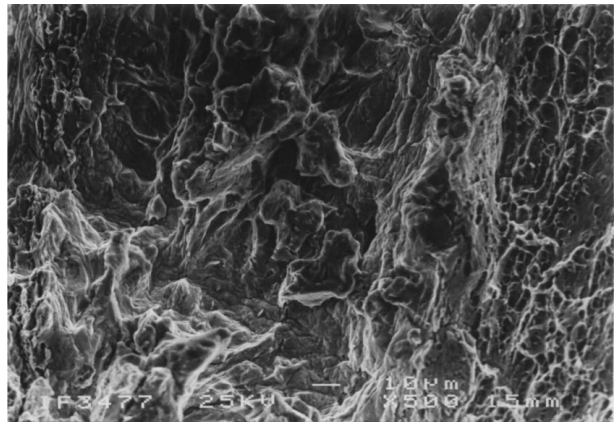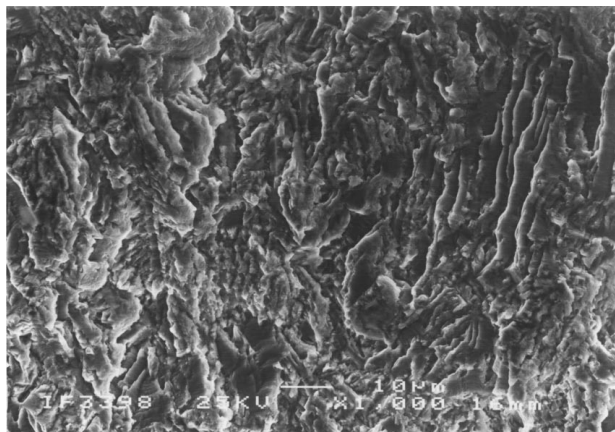
687
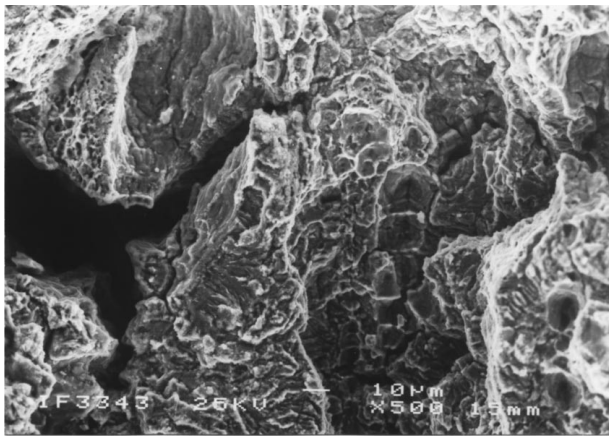
(a)
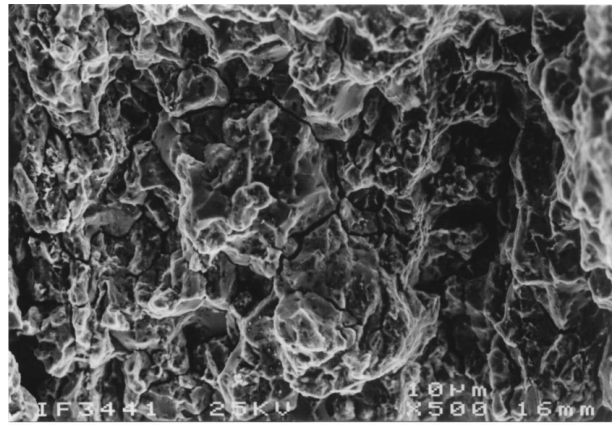
(a)
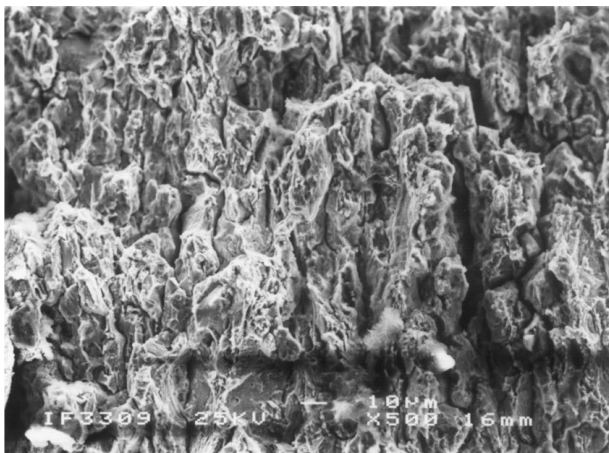
(b)

(b)

Figure 3 Fractographs on Inconel 600 under constant load at 250°C exposed to : (a) 0.1 m NaCl, and (b) 0.01 m NaCl.

(c)

Figure 4 Fractographs on Inco.600 under constant load 250°C exposed to: (a) 0.001 m NaCl, (b) 0.001 m NaCl + 0.0001 m Na_2SO_4, and (c) 0.01 m NaCl + 0.001 m Na_2SO_4.

retardation was observed. However, anodic alloy dissolution by chloride ions at the corrosion potential is accompanied by hydrogen evolution which can penetrate the alloy causing deleterious effects. It is not possible generally to isolate an anodic dissolution type of mechanism from hydrogen related mechanism of intergranular stress corrosion cracking [8]. The hydrogen content of CT-specimens after scc tests was measured; results are shown in Table III. It is clear from the results that hydrogen in the aqueous solution has also a deleterious effect on crack propagation. This seems to confirm that hydrogen enters the material only if a crack is initiated (probably through a dissolution/oxidation process). Hydrogen plays an indirect role, by increasing the plasticity at the crack tip. A very small quantity of hydrogen is sufficient to induce cracking or some microdefects at the grain boundaries. These undergo coalescence when stress is applied, which leads to cracking. The high importance of hydrogen is reported by Jani *et al.* [21] for Inconel 600 and by Englemann *et al.* [5]. Consequently, the difference in crack growth rates in Figs 2, 6, 7 can be recognized as caused by the difference in local environment conditions at a crack tip. In the case of chloride containing sulfate solutions, the crack tip environment seems to be less aggressive than that of chloride ions. Also the hydrogen content near

the crack tip is higher in chloride containing solutions than in solutions with different concentrations of sulfate contents as shown in Table III. A test performed in Na_2SO_4 at 250°C did not show any crack growth. In a few tests the sulfate was added after interrupting the test to evaluate the influence of sulfate (0.1 m) on the growing crack in chloride (0.1 m) environment. The results indicated that the crack did not propagate under this conditions in presence of sulfate. Fig. 8 shows that IGSCC occurred on the region of surface of CT-specimen in 0.1 m chloride but on the other region of
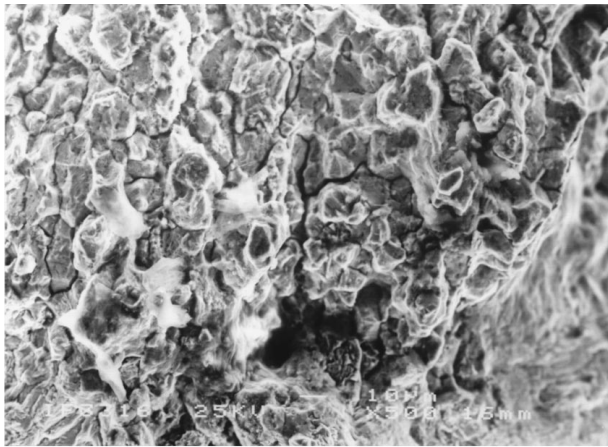
(a)
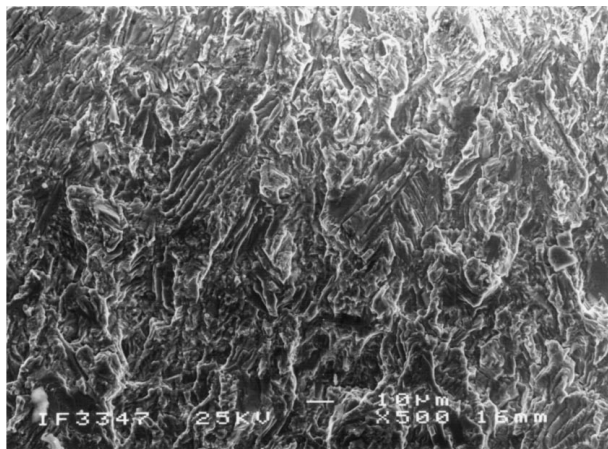
(b)

Figure 5 Fractographs on Inco.600 nuder constant load at 250°C exposed to : (a) 0.01 m NaCl + 0.01 m Na_2SO_4, and (b) 0.01 m NaCl + 0.1 m Na_2SO_4.

the surface IGSCC was less evident and the mode is transfered to transgranular cracking as shown in Fig. 8. Sulfate ions change the morphology of the crack surface from intergranular mode to transgranular failure as representatively shown in Figs 4, 5, 9. Transgranular scc can be interpreted as localized fracture under the sum of the externally applied stress and the stress resulting from the neighboring dislocation pileups laying on different slip planes accumulated in the surrounding slip bands [18]. Fractographic studies have been conducted with a view to understanding the role of the above variables on scc morphology. It has been shown experimentally that chloride ion concentration inside active pits is many times larger than the bulk value [22–24]. Furthermore, if the non aggressive anions are the higher valent species e.g. sulfate ions Vs chloride ion (aggressive ion), the suppression ion concentration and buildup of the non aggressive ion concentration are even greater [25]. Though even as the concentration of sulfate ions increases, the stress intensity factor for Inconel 600 increases. In contrast, fast dissolution by chloride ions around crack tip where no stable film was formed resulted in crack tip blunting. The formation of a blunted crack tip rather than a sharp one caused a reduction in the stress intensity factor [26]. Figs 10,
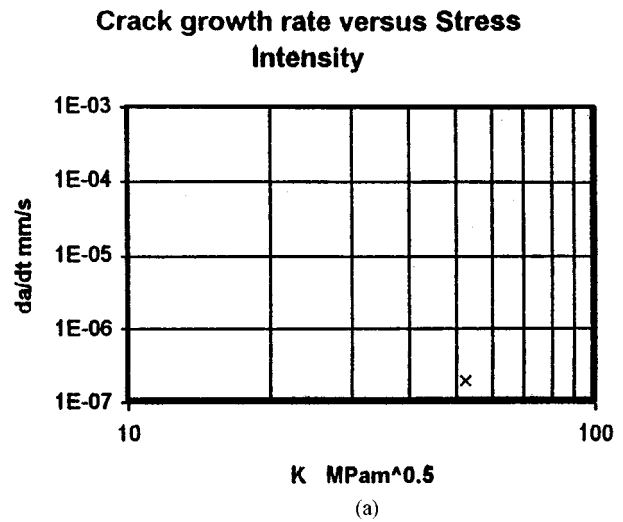
(a)
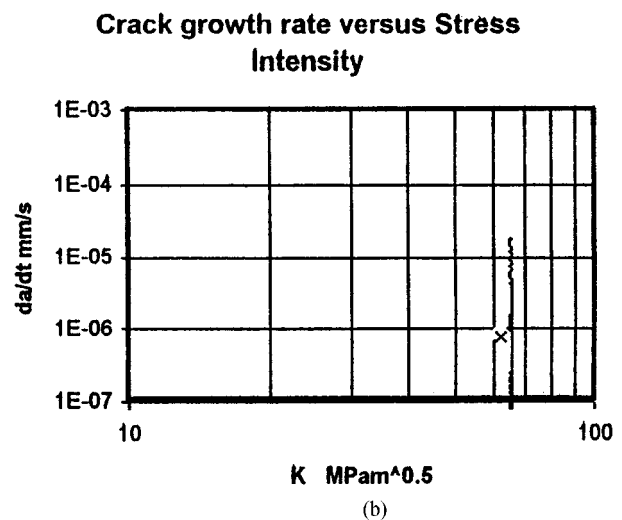
(b)
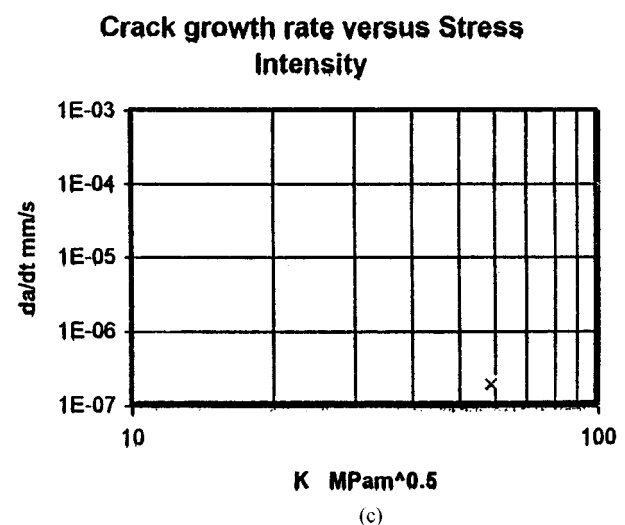
(c)

Figure 6 (a–c) Comparison of crack growth rates Vs Kmax measured in (a) 0.001 m NaCl + 0.0001 m Na_2SO_4, (b) 0.01 m NaCl + 0.001 m Na_2SO_4, and (c) 0.01 m NaCl + 0.01 m Na_2SO_4 under constant load at 8.39 kN at 250°C.

11 show the variation of crack length as a function of time for Alloy 600 tested in constant load conditions in chloride containing sulfate solutions at the open circuit potential at 250°C. However, the resistance of Inco.600 to IGSCC decreased drastically, especially with high concentration of sulfate condition. That means, that
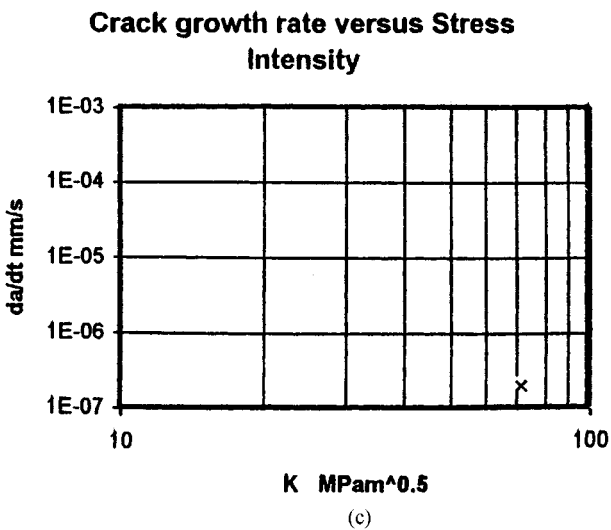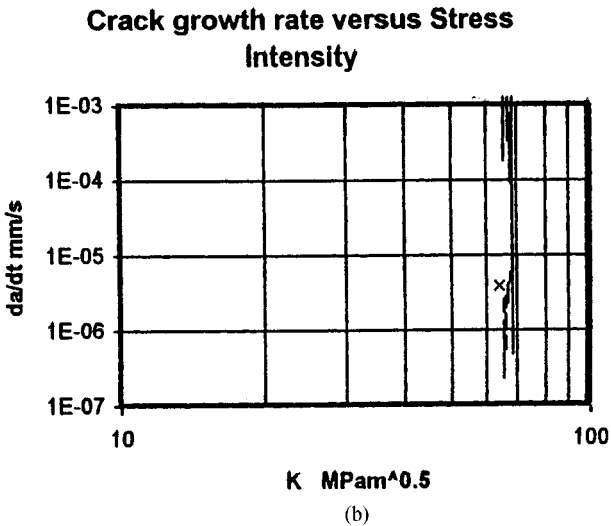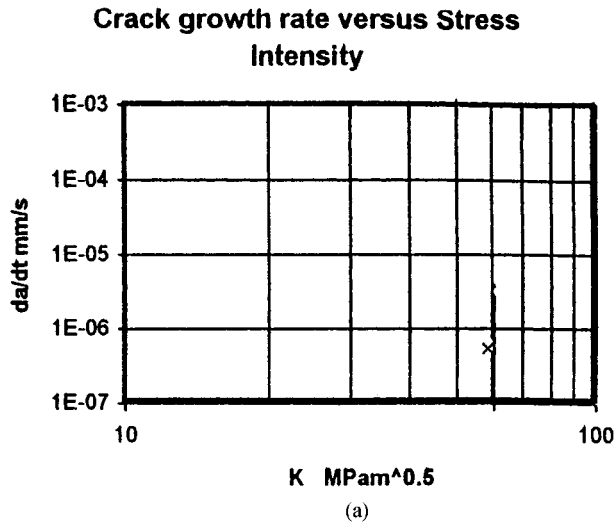
Crack growth rate versus Stress Intensity

(a)

Crack growth rate versus Stress Intensity

(b)

Crack growth rate versus Stress Intensity

(c)

Figure 7 (a–c) Comparison of crack growth rates Vs K max measured in (a) 0.01 m NaCl + 0.1 m Na_2SO_4, (b) 0.1 m Na_2SO_4 and (c) 0.1 m NaCl/0.1 m Na_2SO_4 under constant load at 8.39 kN at 250°C.

(a)

(b)

Figure 8 Fractographs on Inco.600 under constant load at 250°C exposed to 0.1 m NaCl (initiates crack) then add 0.1 m Na_2SO_4 during running test, see text.

Figure 9 Fractographs on Inco.600 exposed to 0.1 m Na_2SO_4 at 250°C under constant load test.

sulfate ions have inhibiting effect on dissolution process by chloride ions for crack initiation which necessary for crack propagation. It is mainly due to a hinderance of chloride ions adsorption on active sites of the fracture surfaces and the formation of chromium oxide layer which is stable at higher temperature. N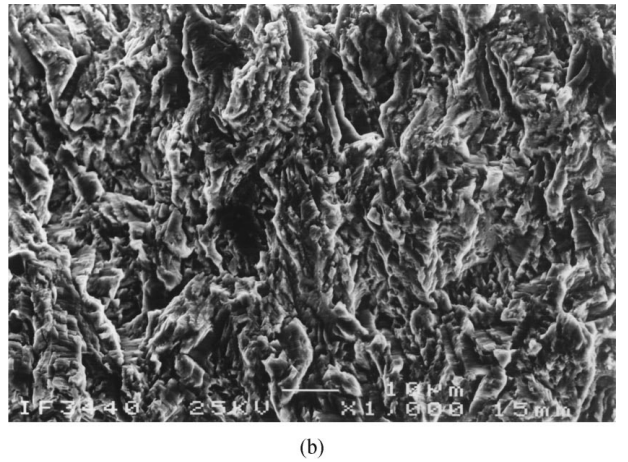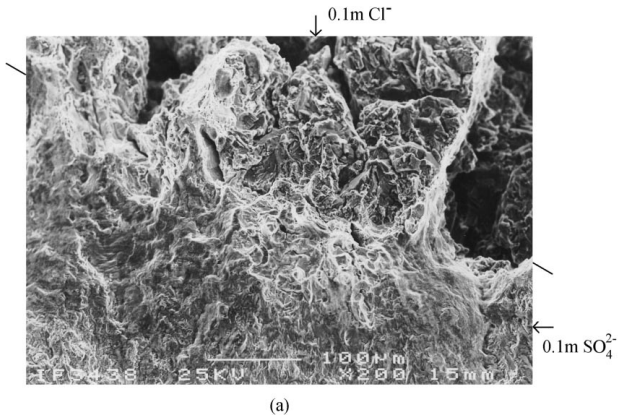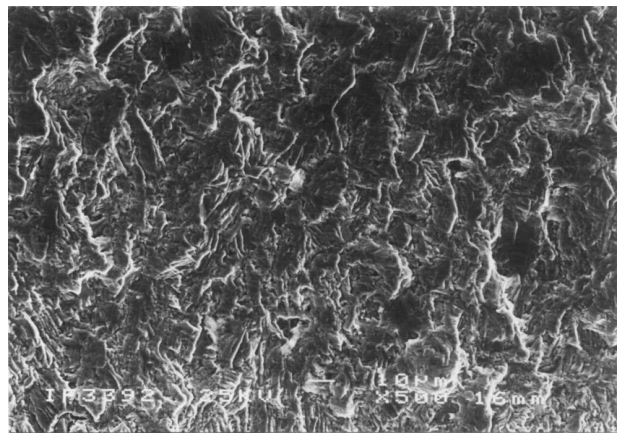everthless, one must consider that many different mechanisms can operate during scc propagation, according to the material-environment systems. Recently, the constant load tests have been analyzed and used for evaluation of scc susceptibility of many materials.
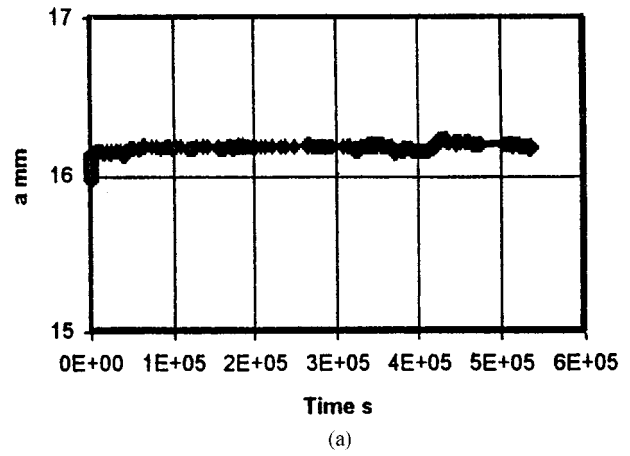
4. Conclusions
The results presented in this paper indicate that :

1. The intergranular stress corrosion crack growth rates increased in chloride solutions while it is hindered by increasing the sulfate concentrations.
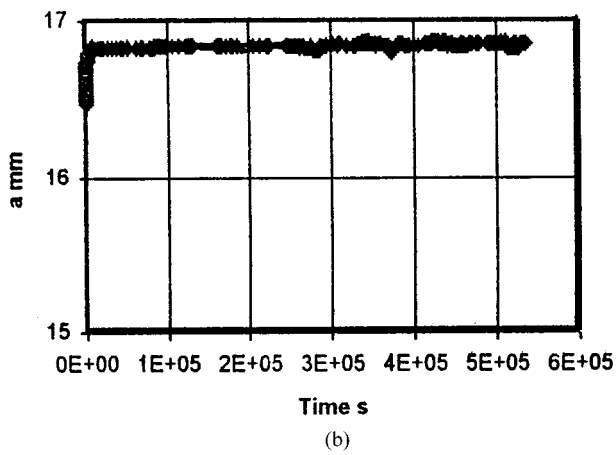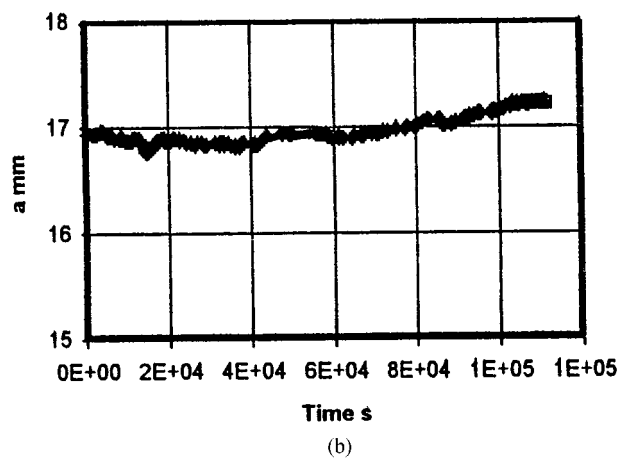
Crack length versus Time
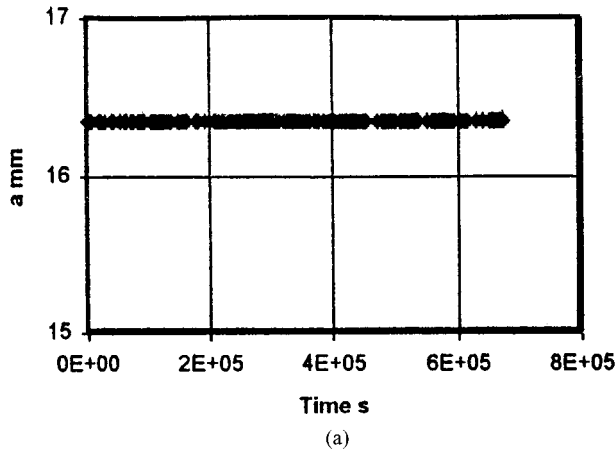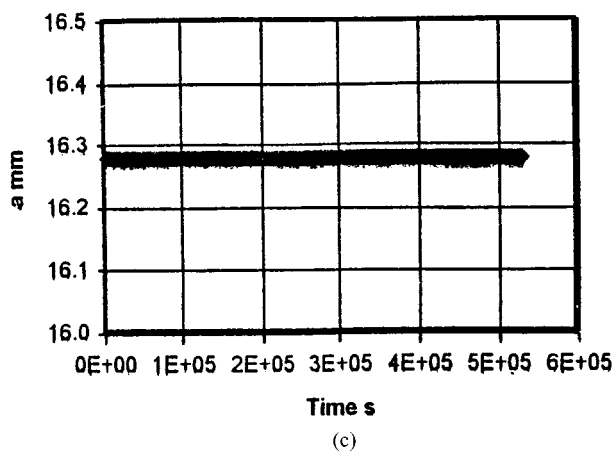

(a)

Crack length versus Time

(b)

Crack length versus Time

(c)

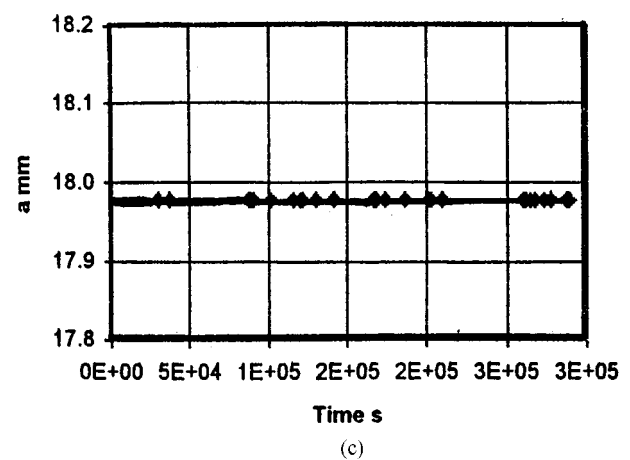*Figure 10* (a–c) Comparison of crack length *a* (mm) Vs time (s) for tests in (a) 0.001 m NaCl + 0.0001 m Na$_2$SO$_4$, (b) 0.01 m NaCl + 0.001 m Na$_2$SO$_4$, and (c) 0.01 m NaCl + 0.01 m Na$_2$SO$_4$ under constant load at 8.39 kN at 250°C.

Crack length versus Time

(a)

Crack length versus Time

(b)

Crack length versus Time

(c)

Figure 11 (a–c) Comparison of crack length *a* (mm) Vs time (s) for tests in (a) 0.01 m NaCl + 0.1 m Na$_2$SO$_4$, (b) 0.1 m Na$_2$SO$_4$ and (c) 0.1 m NaCl/0.1 m Na$_2$SO$_4$ (see text) under constant load at 8.39 kN at 250°C.

2. Stress intensity factor (*K*) decreased with increasing of aggressivity of chloride ions while increased with increasing of concentration of sulfate solutions.

3. Sulfate changed the mode of failure from intergranular to transgranular.

4. The crack doesn't propagate in sulfate solutions with the different concentrations used, under constant load at free corrosion potential.

5. Sulfate hinders the dissolution by chloride ions due to adsorption on active sites of the fracture surfaces

691

and the formation of chromium oxide layer which is stable at high temperature.

Acknowledgements

References

1. E. A. ASHOUR, K. MUMMERT and H.-J. KLAUB, *Werkstoffe und Korrosion* **48** (1997) 151.
2. G. GABETTA, M. M. RADAELLI and M. FERRARI, in 3rd International Atomic Energy Associates (IAEA) Specialists Meeting on Subcritical Crack Growth, Moscow, 14–18 May 1990.
3. R. A. PAGE, A. Mc MINN and S. HUDAK, Jr., *Corrosion* **44** (1988) 623.
4. K. MUMMERT and F. SCHNEIDER, EinfluB von Sulfat auf die HeiBwasserkorrosion von Dampferzeuger-Heizrohren 19. MPA Seminar, Stuttgart, Konf.- Band, Sicherheit und Verfugbarkeit in der Anlagentechnik, 2.A2, Hsgb. K. KuBmaul, Oktober 1993.
5. H. J. ENGELMANN and K. MUMMERT, *Werkstoffe und Korrosion* **43** (1992) 161.
6. *Idem.*, *ibid.* **44** (1993) 454.
7. H. J. ENGELMANN, K. MUMMERT and F. SCHNEIDER, in International Conference on Corrosion – Deformation Interactions, edited by T. Magnin and J. M. Gras (Les Editions de Physique, Les Vlis, 1993) p. 237.
8. R. B. REBAK and Z. SZKLARSKA- SMIALOWSKA, in Proc. of Int. Symp. on Plant Aging and Life Prediction of Corrodible Structures, Sapporo, Japan, May 15–18, 1995, p. AII 15.
9. R. B. REBAK, PhD dissertation, The Ohio State University, 1993.
10. R. B. REBAK and Z. SZKLARSKA – SMIALOWSKA, *Corrosion* **47** (1991) 754.
11. R. B. REBAK, A. R. McILREE and Z. SMIALOWSKA, in 5th Int. Symp. on Environmental Degradation of Materials in Nuclear Power Systems – Water Reactors (La Grange Park, Il. : ANS, 1991) p. 511.
12. M. O. SPEIDEL and R. MAGDOWSKI, in Int. Conf. On Corrosion Deformation Interactions 92 (Les editions de physique, Les Ulys, France, 1992) p. 107.
13. R. B. REBAK and Z. SZKLARSKA – SMIALOWSKA, *Corrosion* **50** (1994) 378.
14. C. H. SHEN and P. G. SHEWMON, *Metallurgical Transactions A* **21A** (1990) 1261.
15. E. A. ASHOUR, F. SCHNEIDER and K. MUMMERT, *Werkstoffe und Korrosion* **48** (1997) 409.
16. "Annual Book of ASTM Standards, Vol. 03.01," (1993) p. 509.
17. G. LEHMANN, K. MUMMERT, M. UHLEMANN and F. SCHNEIDER, in Proc. of the International Atomic Energy Associates (IAEA) Specialists Meeting, Wien (1988) 77 ff.
18. K. LIAN and E. I. MELTIS, *Corrosion* **52** (1996) 347.
19. T. MAGNIN and J. LEPINOUX, in "Proc. Symp. Fundamental Aspects of SCC," edited by S. M. Brummer, E. I. Meletis, R. H. Jones, W. W. Geerberich, F. P. Ford and R. W. Staehle (TMS, Warrendale, PA, 1992) p. 323.
20. A. J. BURSLE, K. R. L. THOMPSON and L. H. KEYS, in "Proc. 6th Int. Cong. Metallic Corrosion" (Mc Graw – Hill Co., Sydney, Australia, 1975) p. 375.
21. S. C. JANI, M. MAAREK, R. F. HOCHMAN and E. I. MELETIS, *Metal. Transact.* **22A** (1991) 1453.
22. Z. SZKLARSKA – SMIALOWSKA, *Corrosion* **27** (1971) 223.
23. T. SUZUKI, M. NAMBE and Y. KITAMURA, *ibid.* **29** (1973) 18.
24. J. MANKOWSKI and Z. SZKLARSKA – SMIALOWSKA, *Corrosion Sci.* **15** (1976) 677.
25. B. G. ATEYA and H. W. PICKERING, in Passivity of Metals, Proc. of the 4th Int. Symp. on Passivity; edited by Robert P. Frankenthal and Jerome Kruger (1978) p. 350.
26. J. B. DUH, W. T. TSAI and J. T. LEE, *Corrosion* **46** (1990) 983.